

Synthesis and Characterization of $\text{Se}_4\text{Nb}_2\text{O}_{13}$: A New Ternary Se^{4+} – Nb^{5+} –Oxide with Monoselenite and Diselenite Groups

P. Shiv Halasyamani* and Dermot O'Hare†

Inorganic Chemistry Laboratory, Oxford University, South Parks Rd., Oxford OX1 3QR, U.K.

Received September 18, 1997. Revised Manuscript Received November 13, 1997

A new noncentrosymmetric ternary selenite, $\text{Se}_4\text{Nb}_2\text{O}_{13}$, has been synthesized from SeO_2 and Nb_2O_5 . Crystal data: $\text{Se}_4\text{Nb}_2\text{O}_{13}$, $M_r = 709.64$, monoclinic, space group Pa (No. 7), $a = 7.555(6)$ Å, $b = 6.637(8)$ Å, $c = 11.377(5)$ Å, $\beta = 109.23(3)^\circ$, $V = 538.64(2)$ Å³ ($T = 200$ K), $Z = 2$, $R(F) = 6.44\%$, $R_w(F) = 7.12\%$. The compound consists of rows of corner-linked NbO_6 octahedra that are also connected through monoselenite, SeO_3 , and diselenite, Se_2O_5 , groups.

Introduction

The synthesis of inorganic compounds that produce second-order nonlinear optical (NLO) responses, e.g., second-harmonic generation (SHG), in combination with chemical and thermal stability, resistance to optical damage, optical transparency, and ease in processing remains vital in developing commercially viable NLO materials.¹ Currently no single inorganic material exhibits all of the above properties for every photonic application (i.e., waveguiding, optical switching, and frequency doubling). Presently mixed-metal oxides, such as LiNbO_3 ,² KTiOPO_4 (KTP),³ and KTP polymorphs⁴ are the primary materials for SHG devices. The large SHG responses observed for these materials are thought to be due to the transition metal–oxygen interactions.^{5–8}

A common feature of all SHG materials is noncentrosymmetry, that is, the material must crystallize in a noncentrosymmetric space group.⁹ To tune the final structure and increase the probability of noncentrosymmetry, as well as maximizing the polarizability in our material, we were careful in selecting the constituent cations. It seemed reasonable therefore to select cations commonly found in asymmetric coordination. The recently reported noncentrosymmetric quaternary sulfides, $\text{La}_6\text{MgGe}_2\text{S}_{14}$ and $\text{La}_6\text{MgSi}_2\text{S}_{14}$, incorporated tet-

rahedrally coordinated Ge^{4+} and Si^{4+} in order to break the inversion symmetry.¹⁰ Other cations, specifically I^{5+} , with nonbonded electron pairs have been discussed by Bergman et al.,¹¹ who determined for the series MIO_3 ($M = \text{H, Li, Na, K, Rb, Cs, NH}_4, \text{ or Tl}$) a nearly 100% incidence of noncentrosymmetry.

We chose to work with Se^{4+} and Nb^{5+} in an attempt to increase the possibility of noncentrosymmetry in our material. The coordination environment of Se^{4+} is intrinsically noncentrosymmetric, with the cation in a distorted tetrahedral environment bonded to three oxygens with the fourth coordination site occupied by the nonbonded electron pair (Figure 1).^{12,13} The second cation we selected, Nb^{5+} , is an octahedrally coordinated d^0 transition metal for which intraoctahedral distortions are often observed. These distortions are thought to be attributable to the second-order Jahn–Teller effect, in which the empty $d\pi$ orbitals of the transition metal mix with the filled $p\pi$ orbital of O^{2-} .^{6,14} We thought by combining two cations found in noncentrosymmetric coordination, the new material would also be noncentrosymmetric and exhibit SHG behavior.

With respect to the d^0 transition metal selenites only $\text{Sc}(\text{HSeO}_3)_3$,¹⁵ Se_2TiO_6 ,¹⁶ $(\text{VO})_2(\text{SeO}_3)_3$,¹⁷ CsVSeO_5 ,¹⁸ $(\text{NH}_4)_2(\text{MoO}_3)_3\text{SeO}_3$,¹⁹ $\text{BaMoO}_3\text{SeO}_3$,²⁰ $\text{BaMo}_2\text{O}_5(\text{SeO}_3)_2$,²⁰ $\text{Cs}_2(\text{MoO}_3)_3\text{SeO}_3$,¹⁹ and $\text{K}_2\text{Se}_2\text{MoO}_8 \cdot 3\text{H}_2\text{O}$ ²¹ have been crystallographically characterized. Interestingly, except

* To whom correspondence should be addressed.

† Royal Society of Chemistry Sir Edward Frankland Fellow.

(1) Marder, S. R.; Sohn, J. E.; Stucky, G. D. *Materials for Non-Linear Optics: Chemical Perspectives*; American Chemical Society: Washington DC, 1991.

(2) Abrahams, S. C.; Reddy, J. M.; Bernstein, J. L. *J. Phys. Chem. Solids* **1966**, *27*, 997.

(3) Tordjman, I.; Masse, R.; Guitel, J. C. *Z. Kristallogr.* **1974**, *139*, 103.

(4) Phillips, M. L. F.; Harrison, W. T. A.; Gier, T. E.; Stucky, G. D.; Kulkarni, G. V.; Burdett, J. K. *Inorg. Chem.* **1990**, *29*, 2158.

(5) DiDomenico, M.; Wemple, S. H. *J. Appl. Phys.* **1969**, *40*, 720.

(6) Goodenough, J. B.; Longo, J. M. *Crystallographic and magnetic properties of perovskite and perovskite-related compounds*; Goodenough, J. B., Longo, J. M., Eds.; Springer-Verlag: Berlin, 1970; Vol. 4.

(7) Lines, M. E. *Phys. Rev. B* **1991**, *43*, 11978.

(8) Kunz, M.; Brown, I. D. *J. Solid State Chem.* **1995**, *115*, 395.

(9) Nye, J. F. *Physical Properties of Crystals*; Oxford University Press: Oxford, 1985.

(10) Gizendanner, R. L.; Spencer, C. M.; DiSalvo, F. J.; Pell, M. A.; Ibers, J. A. *J. Solid State Chem.* **1996**, *131*, 399.

(11) Bergman, J. G.; Boyd, G. D.; Ashkin, A.; Kurtz, S. K. *J. Appl. Phys.* **1969**, *40*, 2860.

(12) Orgel, L. E. *J. Chem. Soc.* **1959**, 3815.

(13) Galy, J.; Meunier, G.; Andersson, S.; Astrom, A. *J. Solid State Chem.* **1975**, *13*, 142.

(14) Wheeler, R. A.; Whangbo, M.-H.; Hughbanks, T.; Hoffmann, R.; Burdett, J. K.; Albright, T. A. *J. Am. Chem. Soc.* **1986**, *108*, 2222.

(15) Valkonen, J.; Leskela, M. *Acta Crystallogr. Sect. B* **1978**, *34*, 1323.

(16) Legros, J.-P.; Galy, J. C. *R. Acad. Sci. Paris* **1978**, *286*, 705.

(17) Halasyamani, P. S.; O'Hare, D. *Inorg. Chem.*, in press.

(18) Kwon, Y.-U.; Lee, K.-S.; Kim, Y. H. *Inorg. Chem.* **1996**, *35*, 1161.

(19) Harrison, W. T. A.; Dussack, L. L.; Jacobson, A. J. *Inorg. Chem.* **1994**, *33*, 3, 6043.

(20) Harrison, W. T. A.; Dussack, L. L.; Jacobson, A. J. *J. Solid State Chem.* **1996**, *125*, 234.

(21) Robl, C.; Haake, K. *J. Chem. Soc., Chem. Commun.* **1992**, 1786.

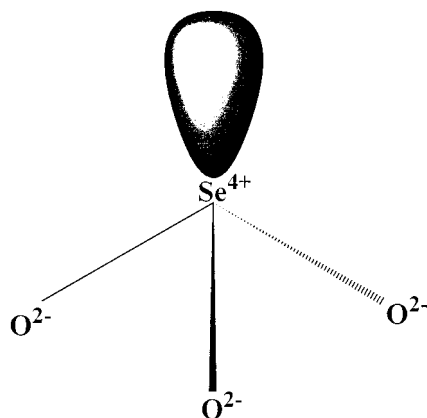


Figure 1. Stick representation of the distorted tetrahedral Se^{4+} coordination environment. The large oval represents the nonbonded electron pair.

for $(\text{VO})_2(\text{SeO}_3)_3$, $\text{BaMoO}_3\text{SeO}_3$, and $\text{K}_2\text{Se}_2\text{MoO}_8 \cdot 3\text{H}_2\text{O}$, all of the above compounds are noncentrosymmetric, suggesting our strategy was reasonable. As recently reviewed,²² the commonly observed selenite groups include SeO_3 , Se_2O_5 , and HSeO_3 . Materials that contain a combination of selenite groups have been synthesized but are fairly uncommon. In fact, only one other compound, $\text{Au}_2(\text{SeO}_3)_2(\text{Se}_2\text{O}_5)$,²³ contains both the monoselenite, SeO_3 , and diselenite, Se_2O_5 , anions.

Here we report the synthesis and characterization of a new noncentrosymmetric ternary selenite, $\text{Se}_4\text{Nb}_2\text{O}_{13}$, that contain SeO_3 , Se_2O_5 , and NbO_6 groups.

Experimental Section

Synthesis of $\text{Se}_4\text{Nb}_2\text{O}_{13}$. *Caution:* Use appropriate safety measures to avoid toxic SeO_2 contamination. $\text{Se}_4\text{Nb}_2\text{O}_{13}$ was synthesized by combining 1.1×10^{-1} g (1×10^{-3} mol) of SeO_2 (Aldrich, 99.9%) with 6.6×10^{-2} g (2.5×10^{-4} mol) of Nb_2O_5 (Aldrich, 99.9%) and adding the mixture into a fused quartz tube. The tube was evacuated, sealed, heated in a furnace at 400°C for 2 days, cooled at 6°C h^{-1} to 300°C , and quenched to room temperature. The tube was opened, and a small irregular shaped faint pink crystal, suitable for single-crystal X-ray diffraction, was extracted. Powder X-ray diffraction on the remaining material resulted in good agreement with the simulated powder pattern for $\text{Se}_4\text{Nb}_2\text{O}_{13}$.

Crystallography. The structure of $\text{Se}_4\text{Nb}_2\text{O}_{13}$ was determined by standard crystallographic methods: A clear light pink crystal was mounted on a thin glass fiber with paratone, and low-temperature [200.0(5) K] data were collected on an image-plate Enraf-Nonius DIP 2000 diffractometer using graphite-monochromated $\text{Mo K}\alpha$ radiation. Ninety frames at 2° steps yielded 7020 reflections ($\theta_{\text{max}} = 26^\circ$) of which 1222 were unique and 769 were observed with $I > 5\sigma(I)$. Indexing was performed by using the program DENZO,²⁴ and data merging was done by using the program SCALEPACK.²⁴ Friedel pairs were not merged, and anomalous dispersion terms were included during the refinements. A DIFABS²⁵ absorption correction was made as well as corrections for Lorentz and polarization effects.²⁶

The crystal structure of $\text{Se}_4\text{Nb}_2\text{O}_{13}$ was solved in space group Pa (No. 7) with initial heavy-atom positions, selenium and

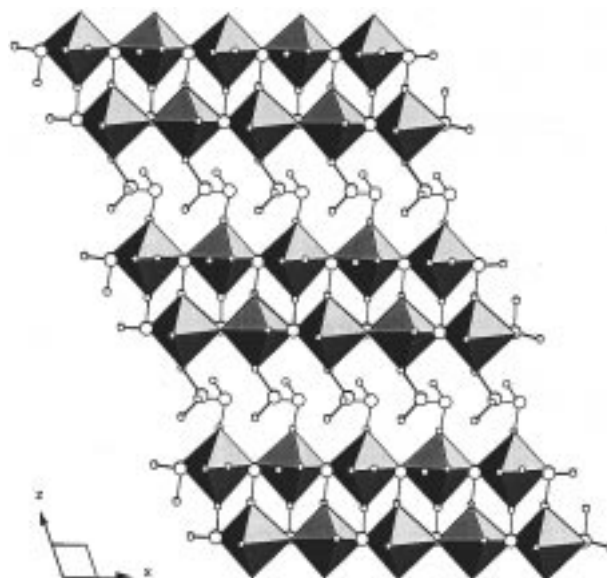


Figure 2. Polyhedral and ball-and-stick representation of $\text{Se}_4\text{Nb}_2\text{O}_{13}$. The Nb^{5+} and Se^{4+} are shown as stippled octahedra and large open circles, respectively.

niobium, located by direct methods by using SIR92.²⁷ A Chebyshev weighting scheme²⁸ was applied during the refinement. The oxygens were located by subsequent cycles of refinements and Fourier difference maps. The final full-matrix least-squares refinement was against F and included anisotropic thermal parameters for Se and Nb and isotropic parameters for oxygen. The final refinement was based on 769 reflections and 107 variable parameters and converged with $R(F) = 0.0644$ and $R_w(F) = 0.0715$. The maximum and minimum peaks on the final difference map corresponded to -2.05 and $+1.76 \text{ e}^-/\text{\AA}^3$, respectively. A symmetry analysis of the $\text{Se}_4\text{Nb}_2\text{O}_{13}$ by using the MISSYM²⁹ program revealed no missing symmetry. All crystallographic calculations were performed using the Oxford CRYSTALS system³⁰ running on a Silicon Graphics Indigo R4000 computer. Crystallographic data, atomic coordinates and thermal parameters, and selected bond distances for $\text{Se}_4\text{Nb}_2\text{O}_{13}$ are given in Tables 1–3, respectively. Two major factors contributed to the relatively large observed errors in the crystal structure. First, the crystal selected for diffraction, the best of a series, had a high mosaicity spread. Second, we were unable to adequately correct the image-plate data for absorption.

Thermogravimetric Analysis. TGA measurements on $\text{Se}_4\text{Nb}_2\text{O}_{13}$ powder revealed one weight loss over a broad range of ca. $350\text{--}500^\circ\text{C}$, corresponding to a loss of 61.4%. Calculated loss for complete SeO_2 elimination 62.5%. Powder XRD showed the remaining powder to be Nb_2O_5 .

Results

A representation of $\text{Se}_4\text{Nb}_2\text{O}_{13}$ is shown in Figure 2. Each Nb^{5+} is octahedrally coordinated to six oxygens (see Table 2). Nb(1) is bonded to O(1), O(2), O(3), O(4), O(5), and a symmetry-equivalent O(5), whereas Nb(2) is linked to O(6), O(7), O(8), O(9), O(10), and a symmetry-equivalent O(10). The bond distances range from 1.77(3) to 2.14(3) \AA for Nb(1), and 1.75(4) to 2.16(4) \AA for Nb(2). The octahedra are corner linked through O(5)

(22) Halasyamani, P. S.; O'Hare, D., *in preparation*.

(23) Jones, P. G.; Schwarzmann, E.; Sheldrick, G. M.; Timpe, H. Z. *Naturforsch.* **1981**, *36b*, 1050.

(24) Otwinowski, Z. *Data Collection and Processing, Proceedings of the CCP4 study weekend*; Daresbury Laboratory: Warrington, 1993.

(25) Walker, N.; Stuart, D. *Acta Crystallogr. Sect. A* **1983**, *39*, 159.

(26) North, A. C. T.; Phillips, D. C.; Matthews, F. S. *Acta Crystallogr. Sect. A* **1968**, *24*, 351.

(27) Altomare, A.; Cascarano, G.; Giacovazzo, C.; Guagliardi, A.; Polidoro, G.; Burla, M. C.; Camalli, M. *J. Appl. Crystallogr.* **1994**, *27*, 435.

(28) Larson, A. C. *Acta Crystallogr.* **1967**, *23*, 664.

(29) Le Page, Y. *J. Appl. Crystallogr.* **1988**, *21*, 983.

(30) Carruthers, J. R.; Watkin, D. J. *CRYSTALS User Manual*; Oxford University Computing Centre: Oxford, 1975.

Table 1. Crystal Data and Structure Refinement for $\text{Se}_4\text{Nb}_2\text{O}_{13}$

formula	$\text{Se}_4\text{Nb}_2\text{O}_{13}$
fw	709.64
space group	Pa (No. 7)
a (Å) ^a	7.555(6)
b (Å)	6.637(8)
c (Å)	11.377(5)
β , deg	109.23(3)
V (Å ³)	538.64(2)
ρ_{calcd} (g cm ⁻³)	4.38
Z	2
T (K)	200.0(5)
μ (cm ⁻¹)	155
$R(F)$	0.064
$R_w(F)$	0.071
Flack enantiopole	0.5(1) ^b

^a The cell constants were obtained from each recorded image and constrained so that $\alpha = \gamma = 90^\circ$. The unit cell constants are mean values with the esds resulting from an analysis of the measurement's consistency. ^b See text.

Table 2. Positional and Displacement Parameters for $\text{Se}_4\text{Nb}_2\text{O}_{13}$

atom	x	y	z	$U(\text{eq})$ (Å ²) ^a
Nb(1)	-0.3208(8)	0.9952(8)	0.0487(5)	0.0129(2) ^b
Nb(2)	-0.4391(8)	0.5094(8)	-0.6025(5)	0.0153(2) ^b
Se(1)	-0.0840(9)	0.4464(8)	0.0607(5)	0.0131(3) ^b
Se(2)	-0.1730(8)	0.9477(8)	0.3856(6)	0.0140(2) ^b
Se(3)	-0.5467(8)	0.9304(6)	-0.2768(5)	0.0161(2) ^b
Se(4)	-0.3901(9)	0.4845(7)	-0.2897(6)	0.0178(2) ^b
O(1)	-0.283(5)	0.988(6)	0.229(3)	0.020(7)
O(2)	-0.271(5)	0.286(5)	0.055(3)	0.014(8)
O(3)	0.071(4)	0.288(4)	0.044(3)	0.003(6)
O(4)	-0.445(5)	0.021(6)	-0.135(3)	0.025(9)
O(5)	-0.095(4)	0.926(5)	0.053(3)	0.018(8)
O(6)	0.002(6)	0.491(6)	0.213(4)	0.028(8)
O(7)	-0.504(6)	0.218(6)	-0.624(4)	0.03(1)
O(8)	-0.339(7)	0.788(7)	-0.594(4)	0.03(1)
O(9)	-0.320(4)	0.471(5)	-0.418(3)	0.013(8)
O(10)	-0.161(6)	0.424(7)	-0.594(4)	0.03(1)
O(11)	-0.361(6)	0.758(7)	-0.277(4)	0.031(8)
O(12)	-0.206(5)	0.423(5)	-0.184(3)	0.031(8)
O(13)	0.002(5)	0.889(5)	0.630(3)	0.024(7)

^a $U(\text{eq})$ is defined as one-third of the trace of the orthogonalized U_{ij} tensor. ^b These atoms were refined anisotropically.

Table 3. Selected Bond Lengths (Å) for $\text{Se}_4\text{Nb}_2\text{O}_{13}$

Nb(1)–O(1)	1.97(3)	Se(1)–O(2)	1.73(4)
Nb(1)–O(2)	1.98(3)	Se(1)–O(3)	1.64(3)
Nb(1)–O(3)	2.04(3)	Se(1)–O(6)	1.67(4)
Nb(1)–O(4)	1.99(3)	Se(2)–O(1)	1.72(4)
Nb(1)–O(5)	1.77(3)	Se(2)–O(7)	1.74(4)
Nb(1)–O(5)*	2.14(3)	Se(2)–O(8)	1.69(4)
Nb(2)–O(6)	1.99(4)	Se(3)–O(4)	1.66(4)
Nb(2)–O(7)	2.01(4)	Se(3)–O(11)	1.83(4)
Nb(2)–O(8)	1.99(4)	Se(3)–O(13)	1.69(3)
Nb(2)–O(9)	2.01(3)	Se(4)–O(9)	1.71(3)
Nb(2)–O(10)	2.16(4)	Se(4)–O(11)	1.82(5)
Nb(2)–O(10)*	1.75(4)	Se(4)–O(12)	1.56(4)

and O(10), in a Nb(1)–O(5)–Nb(1)–O(5) and Nb(2)–O(10)–Nb(2)–O(10) manner, to form rows parallel to the x -axis. Both the Nb(1) and Nb(2) octahedra are also connected through Se(1) and Se(2) selenite groups. Se(1), which is bonded to O(2), O(3), and O(6), connects the Nb(1) octahedra through O(2) and O(3) and bridges the Nb(1) and Nb(2) octahedra through O(6). In a similar manner Se(2), which is bonded to O(1), O(7), and O(8), connects the Nb(2) octahedra through O(7) and O(8) and bridges Nb(1) and Nb(2) through O(1) (see Figure 3). The bond distances of the selenites range

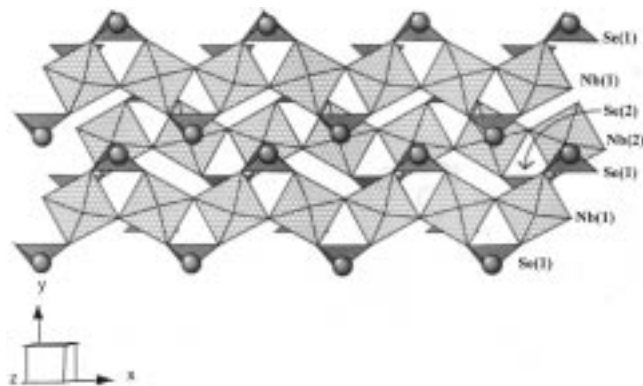


Figure 3. Polyhedral representation of the Nb^{5+} and Se^{4+} interactions. The Nb(1) and Nb(2) octahedra are corner linked as well as connected by the Se(1) and Se(2) selenite groups. The filled circle on the selenium polyhedra represents the nonbonded electron pair.

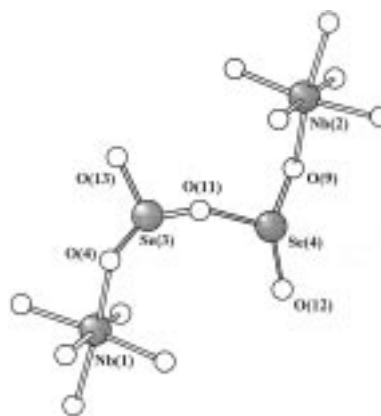


Figure 4. Ball-and-stick representation of the diselenite, Se_2O_5 , moiety that links the rows of niobium octahedra.

from 1.64(3) to 1.73(4) Å for Se(1) and 1.69(4) to 1.74(4) Å for Se(2).

The two remaining selenium atoms, Se(3) and Se(4), form a diselenite group, Se_2O_5 , that bridge the Nb(1) and Nb(2) octahedra (see Figure 4). Se(3) and Se(4) are in similar coordination environments, bonded to three oxygens, two of which, O(4) and O(9), also link to Nb(1) and Nb(2), respectively. O(11) bridges the selenium atoms, whereas O(12) and O(13) are terminal oxygen bonds. The bond distances for the diselenite range from 1.56(4) to 1.83(5) Å. Consistent with other diselenites,^{31–33} the distance to the oxygen that bridges the selenium atoms is longer than the other Se–O distances. For Se(3) and Se(4) the distances to the bridging oxygen, O(11), are 1.83(4) and 1.82(5) Å, respectively. Bond valence³⁴ calculations for $\text{Se}_4\text{Nb}_2\text{O}_{13}$ result in values of 5.22 and 5.23 for Nb(1) and Nb(2), respectively, and 4.48, 4.03, 3.89, and 4.39 for Se(1), Se(2), Se(3), and Se(4), respectively. The oxygen valences range from 1.57 to 2.33.

(31) Meunier, G.; Bertaud, M. *Acta Crystallogr.* **1974**, *B30*, 2840.

(32) Meunier, G.; Svensson, C.; Carpy, A. *Acta Crystallogr.* **1976**, *B32*, 2664.

(33) Hawthorne, F. C.; Groat, L. A.; Ercit, T. S. *Acta Crystallogr.* **1987**, *C43*, 2042.

(34) Brown, I. D.; Altermatt, D. *Acta Crystallogr.* **1985**, *B41*, 244.

Discussion

As previously stated each Nb^{5+} is octahedrally coordinated, forming rows of corner-linked octahedra parallel to the x -axis. In addition, the octahedra are also connected through Se(1) and Se(2) selenite groups. Thus each Nb^{5+} octahedra is bonded to six, two-coordinate oxygens, forming a $[\text{NbO}_6/2]^-$ anion, whereas Se(1) and Se(2) are linked to three, two-coordinate oxygens, forming a $[\text{SeO}_3/2]^+$ cation. The nonbonded electron pairs for both Se(1) and Se(2) are staggered throughout the structure (Figure 3). Along the x -axis, the electron pairs alternate between the $[0\ 1\ 0]$ and $[0\ -1\ 0]$ directions on adjacent selenium atoms.

An interesting feature of $\text{Se}_4\text{Nb}_2\text{O}_{13}$ is the diselenite group. For most of the known diselenites, a Se_2O_5 group is observed where four oxygens link to a second metal and the fifth bridges the selenium atoms. With the diselenite in $\text{Se}_4\text{Nb}_2\text{O}_{13}$, only two of the oxygens bridge to niobium, with a third connecting Se(3) to Se(4). The remaining two oxygens, one on each selenium, are terminal. $\text{Se}_4\text{Nb}_2\text{O}_{13}$ is only the second example of a mixed-metal selenite that contains both monoselenite, SeO_3 , and diselenite, Se_2O_5 , groups. The other example, $\text{Au}_2(\text{SeO}_3)_2(\text{Se}_2\text{O}_5)$,²³ includes a diselenite group with identical coordination to $\text{Se}_4\text{Nb}_2\text{O}_{13}$.

We stated earlier that our motivation for selecting Se^{4+} and Nb^{5+} was to synthesize a noncentrosymmetric material. In this regard we have been successful, since $\text{Se}_4\text{Nb}_2\text{O}_{13}$ crystallizes in the noncentrosymmetric space group Pa . However, preliminary SHG tests on $\text{Se}_4\text{Nb}_2\text{O}_{13}$ powder were not encouraging. When the sample was irradiated with 1064 nm light, no SHG was visible. With this type of powder test green light (532 nm) should have been produced. The question of why no SHG was observed seems relevant.

Two separate reasons can be given for the null SHG response, one structural and the other crystallographic. The structural reason can be appreciated by examining Figure 5, which shows the two rows of Nb^{5+} octahedra. Both Nb(1) and Nb(2) are axially intraoctahedrally distorted, with the difference between the "short" and "long" bond being 0.40 and 0.37 Å, respectively. Compared to LiNbO_3 ,² where the analogous difference is 0.223 Å, suggests that $\text{Se}_4\text{Nb}_2\text{O}_{13}$ should have produced a substantial SHG response. However, as seen in Figure 5, the intraoctahedral distortions are aligned in an antiparallel manner. Any SHG produced by one row of niobium octahedra is "canceled" by the adjacent row. The crystallographic explanation for the null SHG

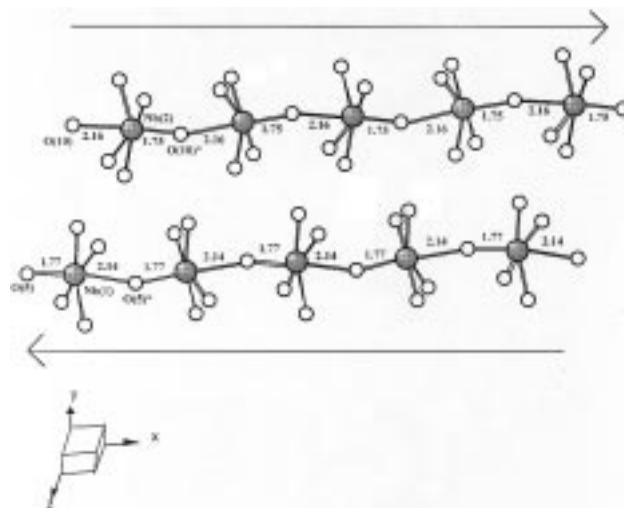


Figure 5. Ball-and-stick representation of the rows of the Nb(1) and Nb(2) corner linked octahedra, with the arrows representing the direction of the distortions. Note the net cancellation of the Nb–O distortions between the rows.

response is inferred from the value of the Flack enantiopole,³⁵ which refined to a value of 0.5(1).³⁶ This value suggests the crystal is twinned, specifically a merohedral twin of class I.³⁷ Since for class I the twin operation belongs to the same Laue group of the crystal, the structural determination was not hindered, however, with respect to the null SHG response, any SHG produced by one "twin" if effectively canceled by the other.

Acknowledgment. The authors wish to thank Dr. Pam Thomas and Dr. Martin Womersley of the University of Warwick for the SHG measurements. Financial support from BNFL (P.S.H.) and the EPSRC is gratefully acknowledged.

Supporting Information Available: An X-ray crystallographic information file, in CIF format (7 pages); structure factors (14 pages). Access and ordering information is given on any current masthead page.

CM970633L

(35) Flack, H. D. *Acta Crystallogr.* **1983**, *A39*, 876.

(36) This refined value should be regarded with caution owing to the quality of the data as well as the fact a DIFABS absorption correction was applied.

(37) Catti, M.; Ferraris, G. *Acta Crystallogr.* **1976**, *A32*, 163.